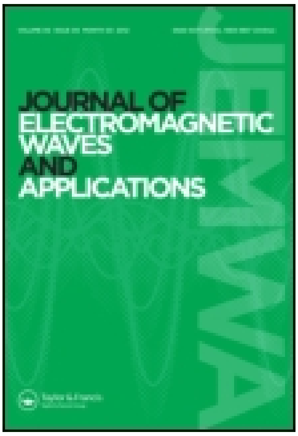

Journal of Electromagnetic Waves and Applications
Publication details, including instructions for authors and subscription information:
http://www.tandfonline.com/loi/tewa20

Design and implementation of compact microwave components with artificial transmission lines

F. Tan [a] , W. Huang [a] , Y. Chen [a] , Y. Li [a] , K. Huang [a] & C. Liu [a]
[a] School of Electronics and Information Engineering , Sichuan University , Chengdu , 610064 , China
Published online: 20 Nov 2012.

Journal of Electromagnetic Waves and Applications, 2013
Vol. 27, No. 3, 385–395, http://dx.doi.org/10.1080/09205071.2013.747122

Design and implementation of compact microwave components with artificial transmission lines

F. Tan, W. Huang, Y. Chen, Y. Li, K. Huang and C. Liu*

School of Electronics and Information Engineering, Sichuan University, Chengdu 610064, China

(*Received 3 August 2012; accepted 19 October 2012*)

In this paper, designs and implementations of a compact diplexer, a broadband balun, and a tight-coupling directional coupler based on artificial transmission lines are presented. Techniques of applying artificial transmission lines to microwave component designs are explored and discussed. All designs show good performance in their respective groups and particularly small circuit sizes at lower microwave frequencies. Those microwave components are successfully implemented using artificial transmission lines based on conventional design topology. Moreover, feasibility and advantages of artificial transmission lines over conventional microstrip lines in designs of various microwave components at lower frequencies are verified such as diplexers, baluns, and directional couplers. Artificial transmission lines have a bright future in the miniaturization of microwave components.

1. Introduction

In recent years, electromagnetic metamaterials have been widely developed in various applications to achieve demanded performances such as to miniaturize microwave components [1–6]. Using curved or bended microstrip lines is the most direct way to miniature microwave circuits. However, the curved microstrip lines can only miniaturize microwave components to a certain extent, and usually insertion losses would increase due to stronger parasitic effect between adjacent microstrip lines. Recently, Wang et al. have proposed a novel planar artificial transmission line [1], which is easy to be fabricated with small insertion loss and good harmonic suppression while miniaturizing circuit size. Since then this new type of artificial transmission line is widely applied.

This paper mainly focuses on applications of planar artificial transmission lines. The characteristic of a unit planar artificial transmission line cell was analyzed and fabricated for verification. Afterwards, technique of applying artificial transmission line to microwave components was presented with detailed examples.

2. Theory of planar artificial transmission line

A unit cell of planar artificial transmission line and its equivalent lumped-element circuit are shown in Figure 1(a) and (b). As shown in Figure 1, the artificial transmission line consists of quasi-lumped elements to realize various equivalent inductance and capacitance of the equivalent transmission line.

*Corresponding author. Email: cjliu@ieee.org

Referring to Figure 1(b), inductors and capacitors of equivalent lumped circuit can be represented by meandered-line inductors, parallel-plated capacitors, and interdigital capacitors, respectively. According to transmission line theory [7], when the parasitic effects are ignored, the characteristic impedance Z_c and phase constant β_g of a lossless artificial transmission line are given by:

$$Z_c = \sqrt{\frac{L_{\text{tot}}}{C_{\text{tot}}}} \tag{1}$$

$$\beta_g = \omega\sqrt{L_{\text{tot}} \times C_{\text{tot}}} \tag{2}$$

where L_{tot} and C_{tot} represent total value of inductance and capacitance for equivalent circuit of artificial transmission line in Figure 1(b), respectively, while ω is the operating angle frequency. As L_{tot} and C_{tot} may be varied proportionally, the characteristic impedance Z_c remains constant while the phase constant β_g varies correspondently. Therefore, the artificial transmission line can achieve any given characteristic impedance and significantly reduced physical length with required electric length.

Figure 1(b) shows that the artificial transmission line consists of a network of inductors and capacitors, which is equivalent to a low-pass filter. There are some studies on microwave filters [8–15]. A compact low-pass filter originated from a unit of artificial transmission line was designed and fabricated to obtain its transmission characteristics. The designed low-pass filter is based on the prototype of a five-order Chebyshev filter of 0.01 dB ripple with a cut-off frequency at 2.4 GHz, while its schematic diagram is shown in Figure 2(a). The lumped inductor L_3 is replaced by a parallel connection of an inductor and a capacitor based on Equation (3), where ω_c stands for the cut-off angular frequency. Meanwhile, in order to increase the attenuation in the stop band, the resonant frequency of the parallel LC-resonator is set with the first attenuation pole at 2.8 GHz according to Equation (4). L_3' and C_3' can be respectively realized by meandered-line inductor and interdigital capacitor.

$$\frac{1}{\omega_c L_3} = \frac{1}{\omega_c L_3'} - \omega_c C_3' \tag{3}$$

$$\omega_p = \frac{1}{\sqrt{L_3' C_3'}} \tag{4}$$

So detailed equivalent parameters of component are determined by layout of artificial transmission line filter in Figure 2(c), which is an identical structure to an artificial transmission line unit in Figure 2(b).

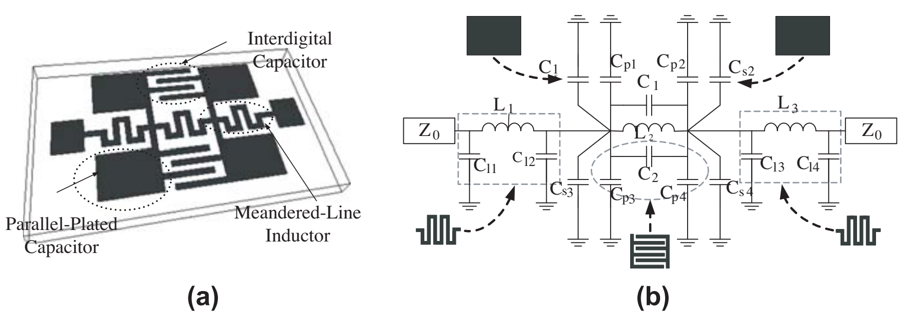

Figure 1. A unit cell of artificial transmission line. (a) Layout of unit cell. (b) Equivalent circuit.

The designed low-pass filter in Figure 3(a) is fabricated on a polytetrafluoroethylene and glass fiber (F4B-2) substrate with relative dielectric constant of 2.65 and loss tangent of 0.003. The size of the fabricated filter is 25 mm × 10 mm, which is $0.3\lambda_g \times 0.11\lambda_g$ measured by the guided wavelength. The proposed filter was measured by an Agilent N5230A

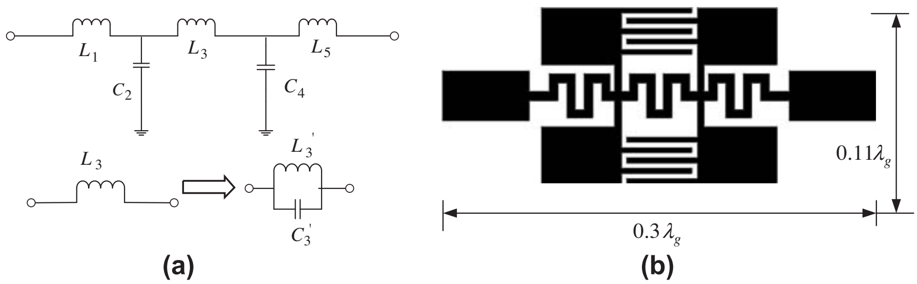

Figure 2. Schematic, layout, and equivalent circuits of the five-order filter based on a unit of artificial transmission line. (a) Schematic of a five-order Chebyshev filter. (b) Layout of the designed filter. (c) Equivalent circuit diagram of the designed filter.

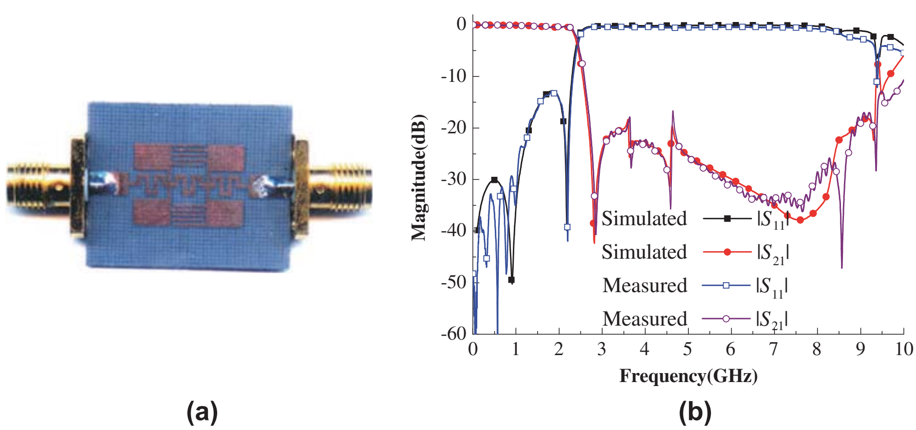

Figure 3. The fabricated low-pass filter and its simulated and measured results. (a) Fabricated low-pass filter. (b) Measured and simulated results.

microwave vector network analyzer. The measured *S*-parameters showed good agreement with the simulations, while some inconformity existed at high frequencies due to fabrication errors.

As shown in Figure 3(b), the measured 3 dB cut-off frequency is 2.42 GHz, while the insertion loss is less than 0.4 dB in the passband and the return loss over 12 dB from DC to 2.2 GHz. The attenuation in the stopband is greater than 17 dB from 2.7 GHz up to 9 GHz with the first attenuation pole at 2.85 GHz, which is also matched with the design initiative. Measured results show that the filter with artificial transmission line owns a compact structure, a steep attenuation, and a wide stopband. Moreover, it depresses the harmonics up to three times greater than its cut-off frequency, which shows advantages over conventional microstrip lines. Therefore, a unit of artificial transmission line can replace a section of conventional transmission line below its cut-off frequency with low insertion loss and reduced physical length.

3. Design of components based on artificial transmission lines

The microwave components are presented as design examples of applications to verify theory analysis of artificial transmission lines. All of the designed components were simulated using software of IE3D, fabricated on a polytetrafluoroethylene and glass fiber (F4B-2) substrate with relative dielectric constant of 2.65 and loss tangent of 0.003, and measured by an Agilent N5230A microwave vector network analyzer.

3.1. Design and implementation of diplexer

The proposed diplexer design is based on the lumped-element schematic diagram of band-pass filtering diplexer shown in Figure 4(a). In this design, two band-pass filters without pass-band overlap are connected together to realize the diplex function and ensure the impedance matching between the filters and the diplexer input port [16]. As shown in Fig. 4(a), a shunt and a series *LC*-resonators are connected together to form two band-pass filtering branches of the diplexer. The schematic diagram in Figure 4(a) can be transferred into topology of distributed lines in Figure 4(b) based on the transmission line theory. $\lambda_g/4$ open-circuit transmission line and $\lambda_g/2$ short-circuit transmission line are used to replace inductors and capacitors of the *LC* resonators in the schematic diagram, where λ_g is the guided wavelength. The designed diplexer achieved impedance matching with transmission lines L_{par1} and L_{par2} according to

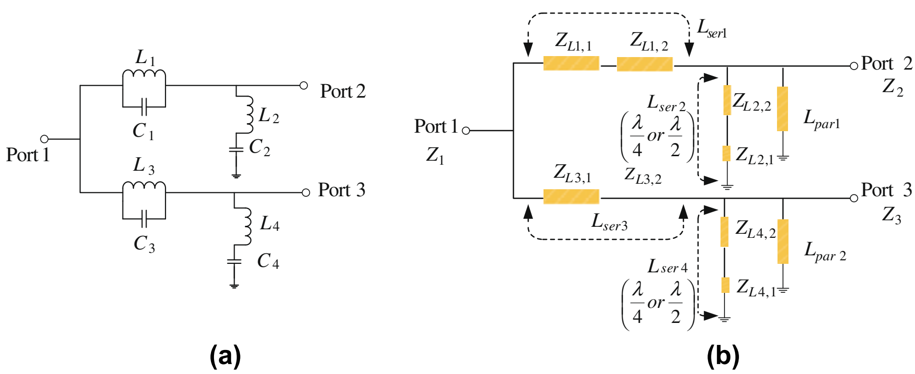

Figure 4. Schematic and transmission line implementation of the diplexer. (a) Schematic diagram of the diplexer. (b) Transmission line implementation.

operating frequencies f_1 and f_2. Using the structure shown in Figure 4(b), diplexers with any operating frequency ratio f_1/f_2 can be realized.

The proposed diplexer operates at 900 and 1800 MHz with a matching impedance of 50 Ω at all three ports. As the operating frequencies of the designed diplexer are 900 and 1800 MHz, operating frequency ratio is 1/2, and the transmission line layout can be simplified as shown in Figure 5(a).

The corresponding layout of the diplexer using artificial transmission lines is shown in Figure 5(b). Characteristic impedance of artificial transmission lines in this design was set to 70 Ω according to the bandwidth considerations, except that the series connected transmission line at port 1 and port 3 were set to 50 Ω for impedance matching. Additionally, short-circuit line was realized by a section of artificial transmission line with a metalized vias.

The dimensions of the diplexer shown in Figure 5(c) are 34 mm × 24 mm, which is $0.16\lambda_g \times 0.11\lambda_g$, where λ_g is the guided wavelength at 900 MHz. As shown in Figure 6, the results show that the insertion loss between ports 1 and 2 at 900 MHz is 26 and 0.05 dB between ports 1 and 3 and that the return losses are 24, 0.5 and 30 dB at ports 1–3, respectively, while isolation between ports 2 and 3 is 42 dB. When operating at 1800 MHz, the insertion loss turns out 0.4 dB between ports 1 and 2, and 20 dB between ports 1 and 3. The respective return losses at ports 1–3 are 18, 19, and 1.8 dB, and isolation between ports 2 and 3 is greater than 28 dB.

The measured results also show that the path from ports 1 to 2 has good transmission at 1800 MHz and fine attenuation at 900 MHz, while the path between ports 1 and 3 does the opposite, and the isolation between ports 2 and 3 achieves an ideal level. The performances indicate that the fabricated diplexer based on artificial transmission lines has satisfied design requirements and demonstrated the design reliability.

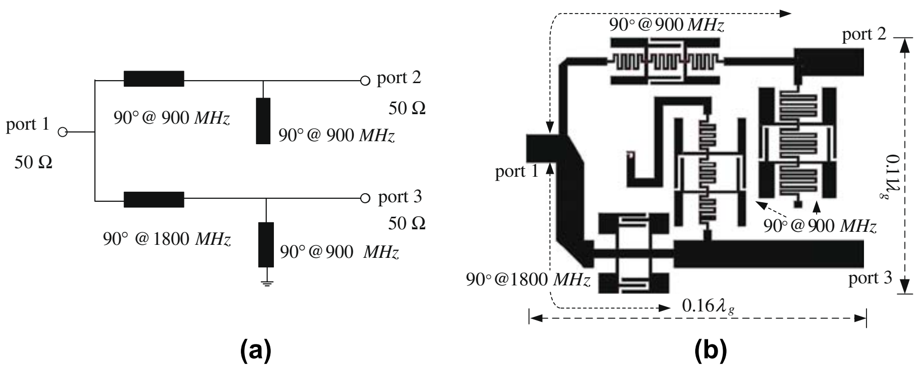

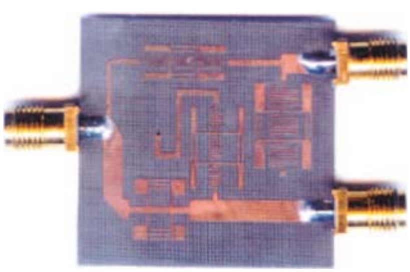

(c)

Figure 5. Artificial transmission line diplexer at 900 and 1800 MHz. (a) Simplified schematic. (b) Artificial transmission line layout. (c) Fabricated diplexer.

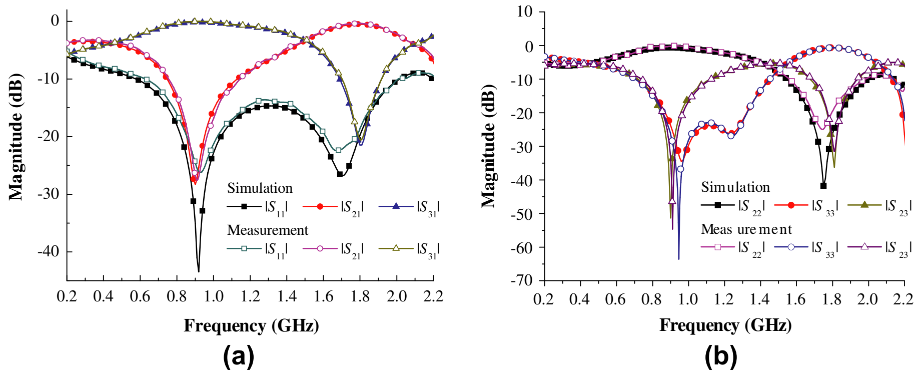

Figure 6. Measured and simulated S-parameters of the proposed diplexer. (a) Transmissions and reflections at input port. (b) Reflections at output ports and isolations.

3.2. *Design and implementation of broadband balun*

A new type of microstrip broadband balun shown in Figure 7 was proposed in [17] beside a few approaches [18,19]. The new structure consists of two parts, a Wilkinson power divider [20–23] and a wideband 180° phase shifter. The power divider splits input power into two halves, and then the wideband phase shifter transfers them into differential signals. In the diagram, Z_a and Z_b stand for input impedances at the terminals; Z_1–Z_4 are characteristic impedance of transmission line sections; and R is the isolation resistance at unbalanced input port. The relations of these parameters are as follows:

$$\begin{aligned} Z_1 &= \sqrt{2Z_a \cdot Z_b} \\ R &= 2Z_b \\ Z_2 &= 1.27Z_b \\ Z_3 &= 1.61Z_b \\ Z_4 &= Z_a = Z_b \end{aligned} \tag{5}$$

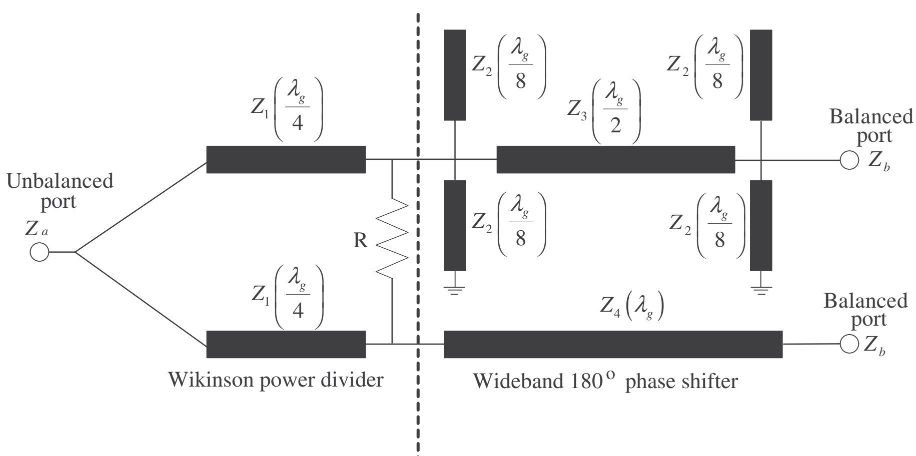

Figure 7. Schematic diagram of the novel broadband balun.

The size of new type of broadband balun implemented with conventional transmission lines would be too large, when applied at low frequencies. In order to reduce the size, planar artificial transmission lines were introduced into the broadband balun design.

Input impedance at three ports was equally set as 50 Ω, that leads the balun parameters to: $Z_1 = 70.7\ \Omega$, $Z_2 = 63.5\ \Omega$, $Z_3 = 80.5\ \Omega$, $Z_4 = 50\ \Omega$, and $R = 100\ \Omega$. Isolation resistance is carried out with a 100 Ω 0603 chip resistor. Artificial transmission line layout of the proposed broadband balun and correspondent impedance together with electrical lengths are shown in Fig. 8(a). The balun circuit size is 90 mm × 62 mm, which is $0.40\lambda_g \times 0.28\lambda_g$ in guided wavelength dimension at 915 MHz. The proposed design with planar artificial transmission lines significantly reduces the circuit size of the balun layout in Fig. 7 up to 35% compared with the original layout with conventional microstrip lines.

Figure 8(b) is a photo of the fabricated broadband balun. The measured *S*-parameters presented in Figure 9 show good agreements with the simulations. At the center frequency of 915 MHz, the insertion loss is 3.7 dB through port 1 to port 2 and 3.6 dB through port 1 to port 3. Besides, the insertion loss is larger than conventional microstrip structures due to multisections of discontinuous structure in the proposed balun. Return losses at ports 1 to 3 are 37, 36, and 37 dB, respectively, and the isolation between ports 2 and 3 is greater than 34 dB.

In the frequency band from 0.65 to 1.1 GHz, the insertion loss is 3.9 ± 0.2 dB between ports 1 and 2, and 3.55 ± 0.15 dB between ports 2 and 3. The return loss is larger than 14 dB at port 1, larger than 10 dB at port 2, and greater than 20 dB at port 3, while isolation between ports 2 and 3 maintains greater than 16 dB. The relative bandwidth is 49%, which is less than 64% of the balun in Figure 7. However, the implemented layout by artificial transmission lines significantly reduces the circuit size and has larger than 38% relative bandwidth of a conventional three-order half-wavelength line balun.

Figure 9(c) shows the phase output of the broadband balun, and the phase difference between two out ports is $180° \pm 6°$ from 0.65 GHz to 1.1 GHz. The broadband response in Figure 9(d) shows insertion loss from input ports to output port is larger than 10 dB from 2.2 to 20 GHz, which sufficiently suppresses harmonics.

3.3. *Directional coupler design with artificial transmission line and D-CRLH-TL*

The composite right-/left-handed transmission line (CRLH TL) is a kind of metamaterial transmission line, which is first proposed by Itoh's group in [5]. A CRLH TL unit is

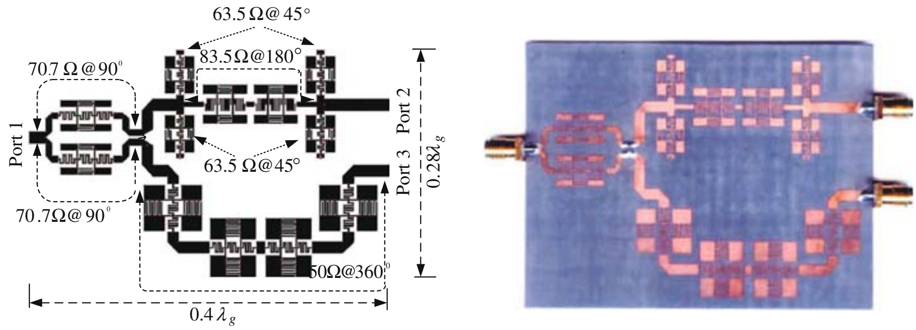

(a) (b)

Figure 8. Broadband balun based on artificial transmission lines. (a) Artificial transmission line layout. (b) The fabricated balun.

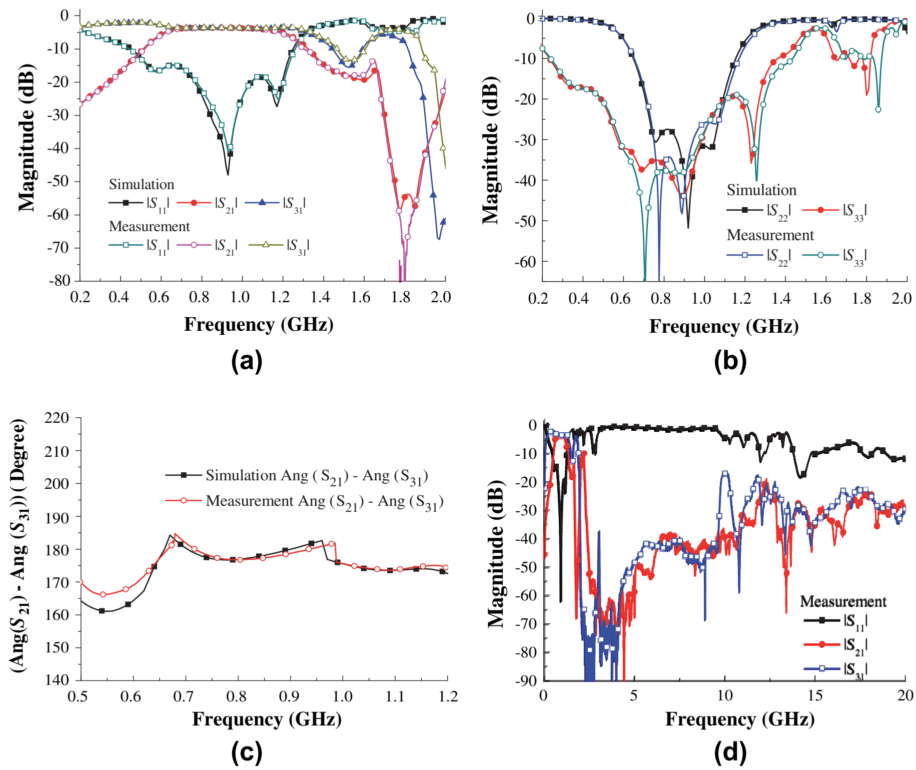

Figure 9. Measured and simulated S-parameters of the proposed broadband balun. (a) Reflections at input port and transmissions. (b) Reflections at output ports. (c) Phase outputs of the designed balun. (d) Broadband response.

equivalent to a series LC-tank and a shunt parallel LC-tank, shows a passband nature, and exhibits both left-handed (LH) and right-handed (RH) characteristics with an LH band at low frequencies and a RH band at high frequencies. Recently, CRLH TLs have found more and more applications in novel microwave components [24,25].

A Dual CRLH TL (D-CRLH TL), of which a unit is equivalent to series parallel LC-tank and shunt series LC-tank, is the "dual" of a conventional CRLH [24]. The D-CRLH TL presents low-frequency LH band, high-frequency RH band, and a stopband nature. Besides, the balanced condition of a CRLH TL is still valid for D-CRLH TL for broadband matching.

The combination of a CRLH TL and artificial transmission line has already been proved efficient in promoting the performance and enhancing the dynamic range of coupled-line directional couplers at low frequencies. In this paper, directional coupler designed with D-CRLH-TL and artificial transmission line is proposed to benefit the coupler performance at high frequencies.

The directional coupler designed with D-CRLH TL and artificial transmission line is presented in Figure 10(a). The input impedance at all ports is equally set to 50 Ω. The D-CRLH TL consists of three cascade connection of D-CRLH TL units and two sections of 50 Ω conventional transmission line at both ends. Figure 10(b) shows the fabricated directional coupler. In order to increase coupling efficiency, straight microstrip lines were applied to take the place of meandered-line inductance. The size of the coupler layout is 14.6 mm × 11.2 mm as shown in Figure 10(b), which is $0.43\lambda_g \times 0.33\lambda_g$ at 5.8 GHz. Port 1

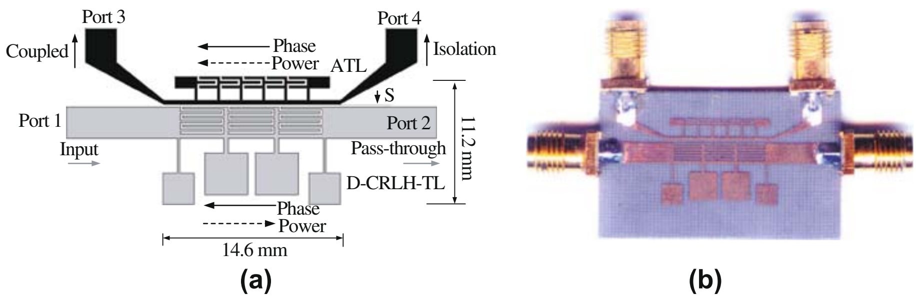

Figure 10. Directional coupler based on artificial transmission lines and D-CRLH. (a) Layout of the directional coupler with artificial transmission lines and D-CRLH. (b) Photo of the fabricated direction coupler.

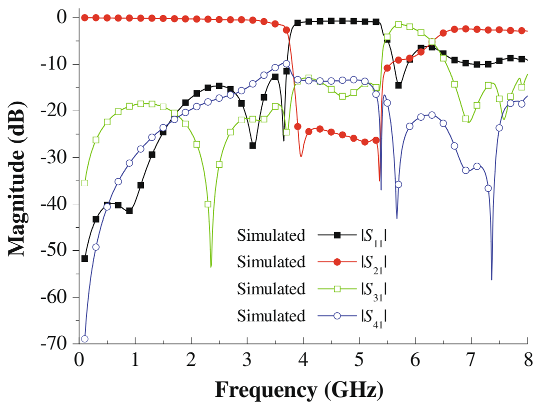

Figure 11. Simulated results of D-CRLH TL and artificial transmission line coupler with $S = 0.1$ mm.

to Port 4 were coincidentally set as input port, pass-through port, coupled port, and isolation port, respectively.

The coupling gap S between D-CRLH TL and artificial transmission line was set to 0.1 mm for simulation. As shown in Figure 11, the results show that coupling coefficient is 1.4 dB for artificial transmission line coupler. Therefore, using artificial transmission line in coupler design can achieve higher coupling coefficient for a certain coupling length. In other words, the artificial transmission lines can effectively reduce the circuit size of a coupler for a certain coupling coefficient.

Based on the above simulation, a 3 dB directional coupler with center frequency of 5.8 GHz was designed and fabricated with a D-CRLH TL and artificial transmission line. The coupling gap S was set as 0.3 mm to accomplish 3 dB coupling coefficient. Figure 10(b) shows the fabricated directional coupler.

Measured and simulated S-parameters of the 3 dB directional coupler are presented in Figure 12, showing good agreements with each other. At 5.8 GHz, the directional coupler has a coupling coefficient of 3.1 dB and isolation of 29 dB. The return loss at the input port is 15 dB, and the insertion loss between port 1 and port 2 is 4.5 dB. The high insertion loss is due to the radiation loss and parasitic effects of discontinuous components in the coupling structure at high frequencies. The coupler maintains the coupling flatness less than 1 dB,

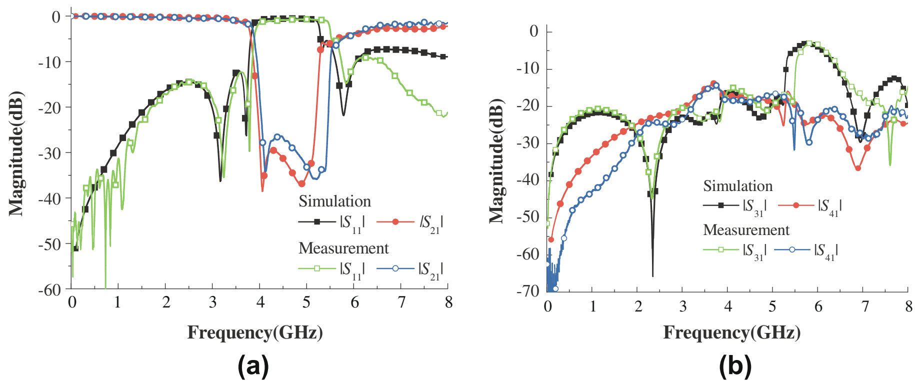

Figure 12. Measured and simulated *S*-parameters of the fabricated coupler. (a) Reflection and pass-through. (b) Coupling and isolation.

isolation over 26 dB, and return loss at port 1 higher than 10 dB over the range from 5.7 to 5.9 GHz.

Measured results of the proposed directional coupler indicate that couplers designed with D-CRLH TL and artificial transmission line have characteristics like tight coupling, backward coupling, good isolation, and small size, compared with couplers designed by conventional transmission lines.

4. Conclusion

The structures, characteristics, and design of planar artificial transmission lines have been discussed and reviewed briefly. The applications of artificial transmission lines to design of microwave components are presented and demonstrated by a few examples, and their significant effect on circuit size miniaturization is verified. The main drawback of artificial transmission lines is the higher insertion loss. These experiments prove that artificial transmission lines are highly applicable to design compact microwave devices at lower microwave frequency band.

Acknowledgments

This work was supported in part by the NFSC 60971051, the Sichuan Youth Foundation 09ZQ026-016 and the Key Laboratory of Cognitive Radio (GUET), Ministry of Education, China.

References

[1] Wang C, Ma T, Yang C. A new planar artificial transmission line and its applications to a miniaturized Butler matrix. IEEE Trans. Microwave Theory Tech. 2007;55:2792–2801.
[2] Liu C, Yang T, Huang K, Menzel W. Compact capacitive compensated directional coupler using planar artificial transmission lines. Electronics Lett. 2011;27:1321–1323.
[3] Huang W, Liu C, Yan L, Huang K. A miniaturized dual-band power divider with harmonic suppression for GSM applications. J. Electromagn. Waves Appl. 2010;24:81–91.
[4] Zhao X, Zhao L, Huang K, Liu C. A circularly polarized array composed of linear polarized microstrip patches fed by metamaterial transmission line. J. Electromagn. Waves Appl. 2011;25:1545–1553.
[5] Lai A, Itoh T, Caloz C. Composite right/left-handed transmission line metamaterials. IEEE Microwave Mag. 2004;5:1527–3342.

[6] Liu C-J, Menzel W. Broadband via-free microstrip balun using metamaterial transmission lines. IEEE Microwave Wireless Compon. Lett. 2008;18:437–439.
[7] Kong JA. Electromagnetic wave theory. Cambridge (MA): EMW Publishing; 2008.
[8] Chen H, Wu Y-H, Yang Y-M, Zhang Y-X. A novel and compact bandstop filter with folded microstrip/CPW hybrid structure. J. Electromagn. Waves Appl. 2010;24:103–112.
[9] Dai G-L, Xia M-Y. An investigation of quarter-wavelength square-spiral resonator and its applications to miniaturized bandpass filters. J. Electromagn. Waves Appl. 2010;24:1303–1313.
[10] He Q, Liu C. A novel low-pass filter with an embedded band-stop structure for improved stop-band characteristics. IEEE Microwave Wireless Compon. Lett. 2009;19:629–631.
[11] Hu G, Liu C, Yan L, Huang K, Menzel W. Novel dual mode substrate integrated waveguide band-pass filters. J. Electromagn. Waves Appl. 2010;24:1661–1672.
[12] Lin H-J, Chen X-Q, Shi X-W, Chen L, Li C-L. A dual passband filter using hybrid microstrip open loop resonators and coplanar waveguide slotline resonators. J. Electromagn. Waves Appl. 2010;24:141–149.
[13] Hu G, Chen Y, Zhao X, Huang K, Liu C. Novel high selective bandpass filters incorporated with quasi-lumped impedance inverters. J. Electromagn. Waves Appl. 2011;25:1382–1390.
[14] Wu Y, Liu Y, Li S, Yu C. A simple microstrip bandpass filter with analytical design theory and sharp skirt selectivity. J. Electromagn. Waves Appl. 2011;25:1253–1263.
[15] Wu Y, Liu Y, Li S, Yu C. A new wide-stopband low-pass filter with generalized coupled-line circuit and analytical theory. Prog. Electromagn. Res. 2011;116:553–567.
[16] Fritz M, Wiesbeck W. A diplexer based on transmission lines, implemented in LTCC. IEEE Trans. Microwave Theory Tech. 2006;29:427–432.
[17] Zhang ZY, Guo YX, Ong LC, Chia M Y W. A new wide-band planar balun on a single-layer PCB. IEEE Microwave Wireless Compon. Lett. 2005;15:416–418.
[18] Yeh Z-Y, Chiang Y-C. A miniature CPW balun constructed with length-reduced 3 dB couples and a short redundant transmission line. Prog. Electromagn. Res. 2011;117:195–208.
[19] Shao W, Li J-L. A compact log-periodic branch-line balun with an octave bandwidth. J. Electro-magn. Waves Appl. 2011;25:2033–2042.
[20] Deng P-H, Guo J-H, Kuo W-C. New Wilkinson power dividers based on compact stepped-imped-ance transmission lines and shunt open stubs. Prog. Electromagn. Res. 2012;123:407–426.
[21] Zhang Z, Jiao Y-C, Tu S, Ning S-M, Cao S-F. A miniaturized broadband 4:1 unequal Wilkinson power divider. J. Electromagn. Waves Appl. 2010;24:505–511.
[22] Huang W, Liu C-J, Chen Q, Li Y-N, Chen X, Huang K-M. Compact unequal Wilkinson power divid-ers using planar artificial transmission lines. J. Electromagn. Waves Appl. 2011;25:2201–2211.
[23] Li B, Wu X, Yang N, Wu W. Dual-band equal/unequal Wilkinson power dividers based on coupled-line section with short-circuited stub. Prog. Electromagn. Res. 2011;111:163–178.
[24] Caloz C. Dual composite right/left-handed (D-CRLH) transmission line metamaterial. IEEE Microwave Wireless Compon. Lett. Nov. 2006;16:585–587.
[25] Wang W, Liu C, Yan L, Huang K. A novel power divider based on dual-composite right/left handed transmission line. J. Electromagn. Waves Appl. 2009;23:1173–1180.